

Supplementary material : velocity model tables

Layer top (km)	V _P (km/s)	V _S (km/s)
0.00	3.58	2.16
0.40	3.58	2.16
1.84	4.95	2.98
3.94	5.15	3.10
7.04	5.81	3.50
11.77	6.19	3.73
20.97	6.64	4.00
42.37	7.30	4.40

Supplementary table 1: ADofal gradient velocity layer model.

Layer top (km)	V _P (km/s)	V _S (km/s)
0.0	2.42	1.41
5.5	2.80	1.63
7.0	3.60	2.09
7.5	5.30	3.08
8.6	6.10	3.55
10.8	7.10	4.13
15.0	8.00	4.65

Supplementary table 2: Coffin449 constant velocity layer model.

Layer top (km)	V _P (km/s)	V _S (km/s)
0.0	5.800	3.46
20.0	5.800	3.46
20.0	6.500	3.85
35.0	6.500	3.85
35.0	8.400	4.48
77.5	8.045	4.49
120.0	8.050	4.50

Supplementary table 3: ak135 constant velocity layer model.

Sediment presence check with P to S conversions

We looked at P-wave converted into S-wave by the basement/sediment interface in order to have some clues about the sediment thickness that could impact the S-arrival times and cause depth resolution problems.

For each sensor of the first deployment, we vertically aligned on the picked P-phase the vertical and horizontal traces of a set of magnitude >3.5 events. The P-wave is most visible on the vertical channel while the P converted to S should be visible on the horizontal channel. Assuming a 200m thick, very low s-wave velocity sediment layer (0.2 km/s) a delay around 1s is expected between the P-wave and its conversion in S-wave. While MOSO (Figure S1f), on the south-west of the area, shows a complicated soil response, we can spot a delay of 1s only on MONE (Figure S1b). On all the other stations, we have delays on the order of 0.5s.

This indicates that the 200m thick, 0.2 km/s low S-wave velocity, sediment layer we tested in our study is the worst case for our study area.

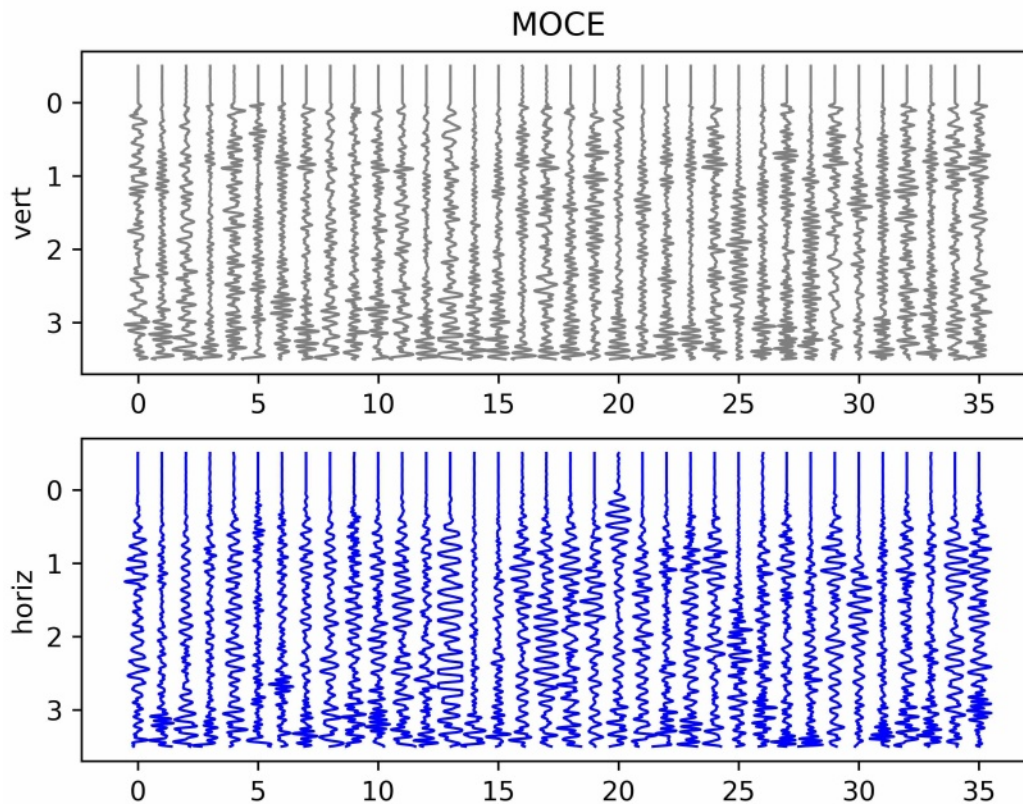


Figure S1a : MOCE (center) station showing delay of approximately 0.5s.

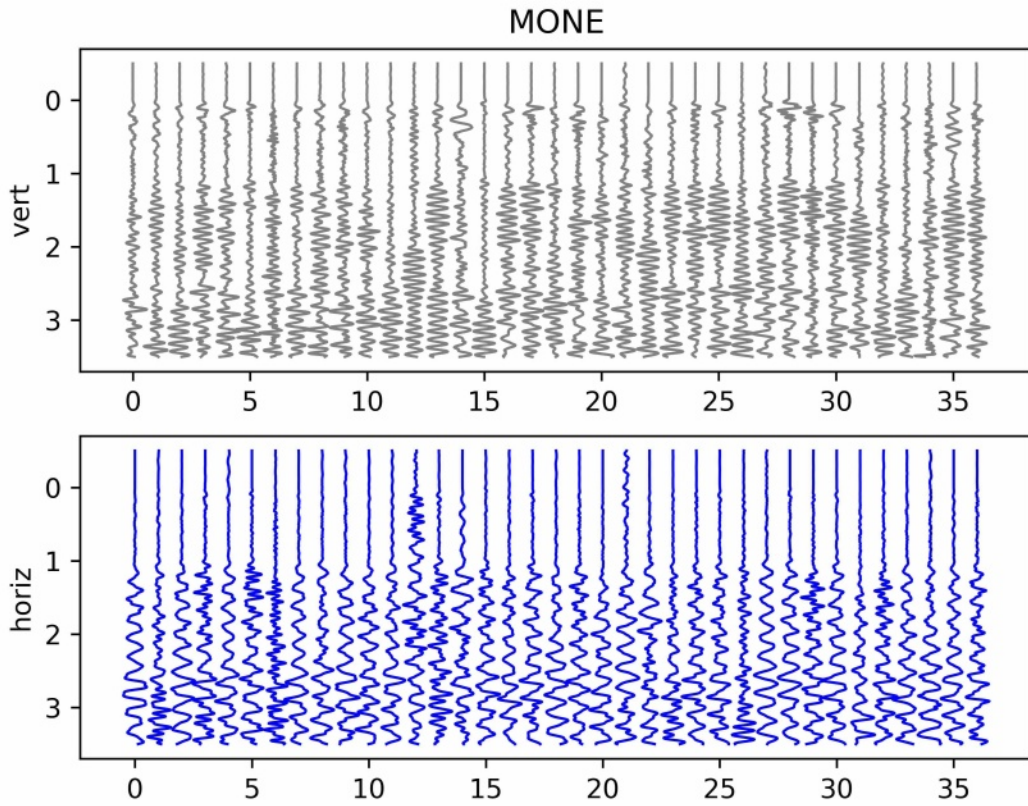


Figure S1b : MONE (north-east) station in the abyssal plain, showing delay of approximately 1s.

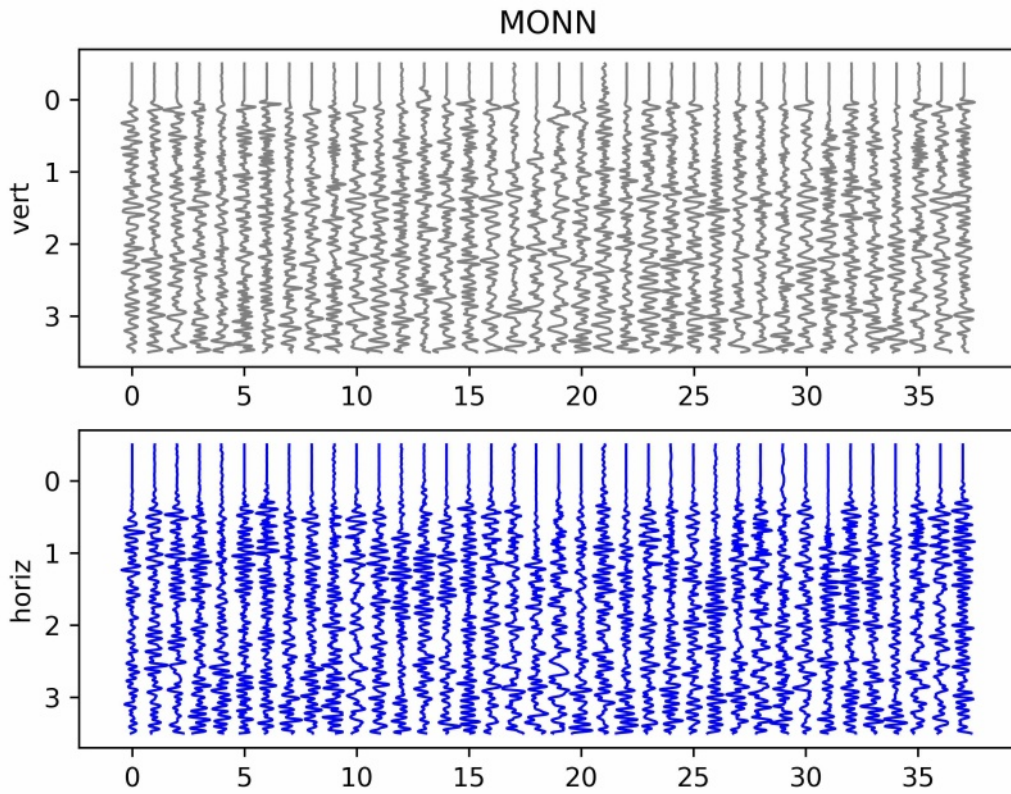


Figure S1c : MONN (north) station, showing delay of approximately 0.5s.

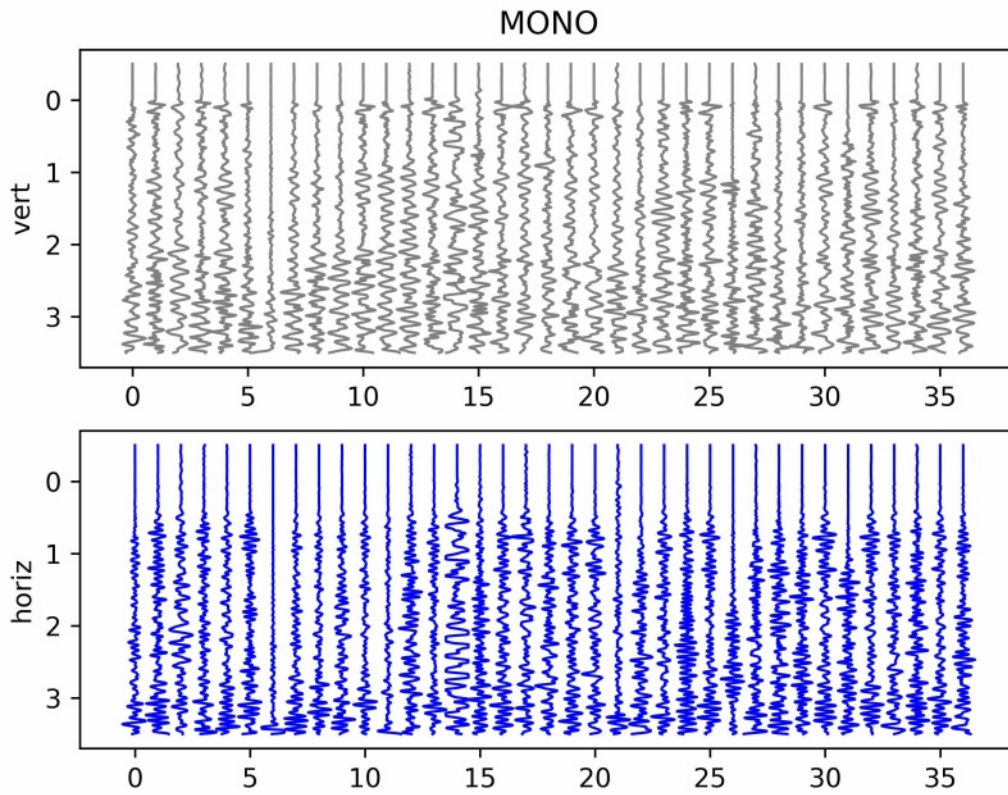


Figure S1d : MONO (north-west) station, showing delay of approximately 0.75s.

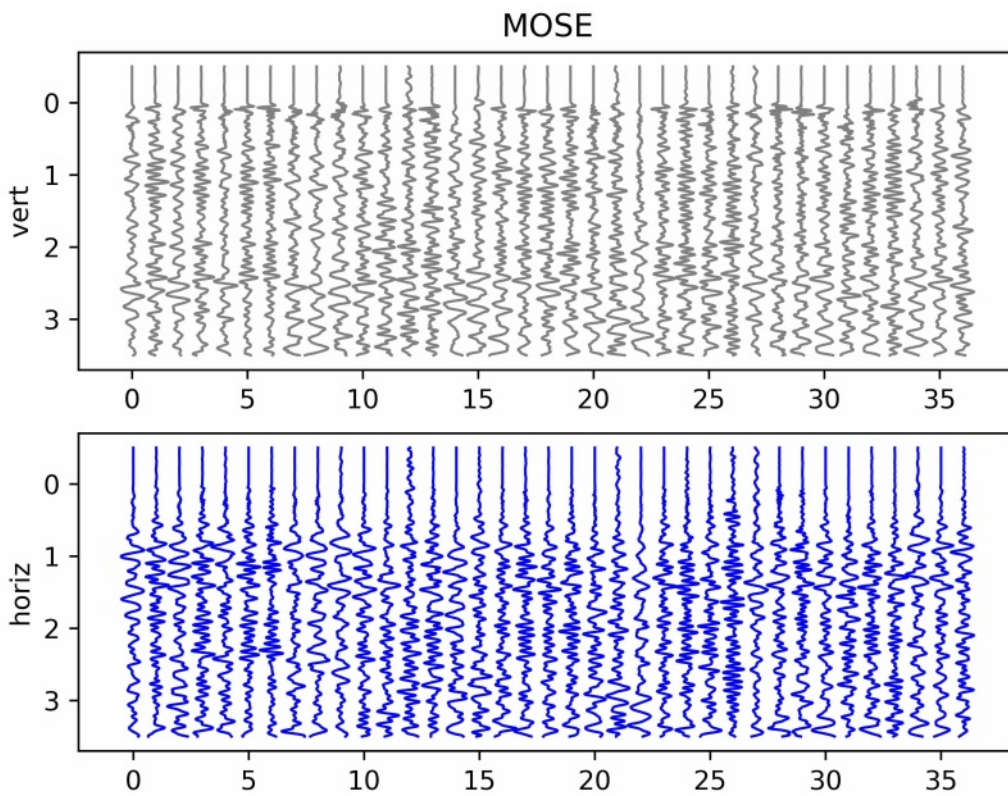


Figure S1e : MOSE (south-east) station, showing delay of approximately 0.5s.

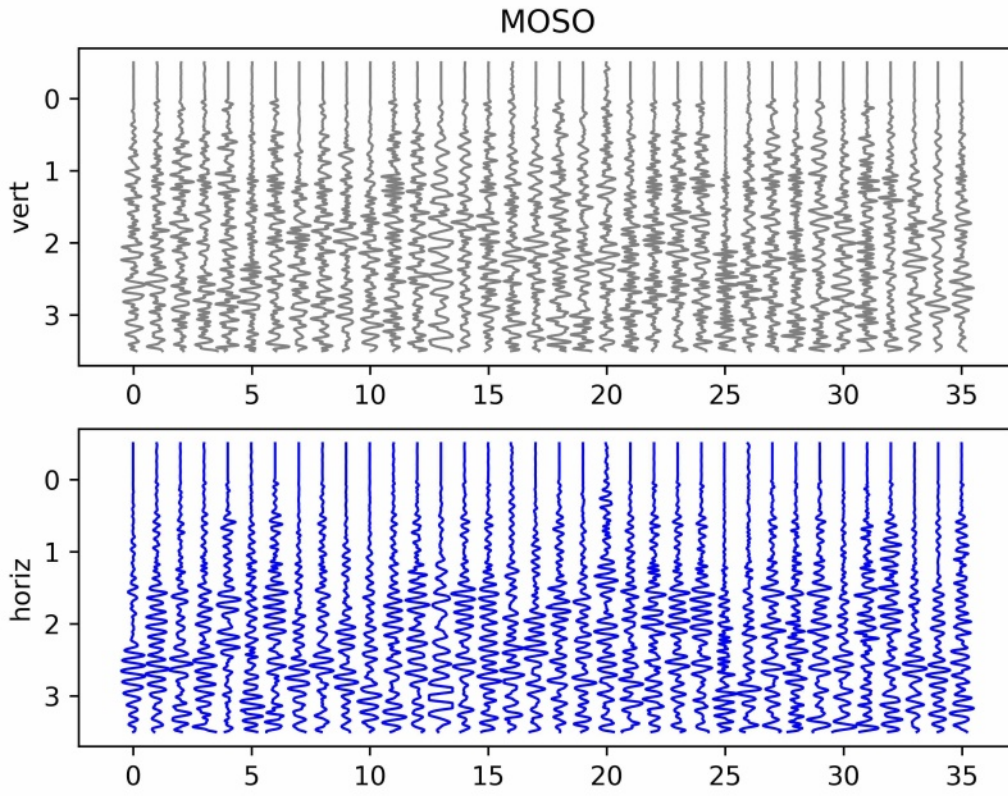


Figure S1f : MOSO (south-west) station, showing a complex conversion response with possible multiple conversions and a first delay of 0.5s.

Comparison with Lemoine et al (2020) catalog

Between February 25th 2019 and May 14th 2019, 308 earthquakes are common to both Lemoine et al (2020) and this study catalogs.

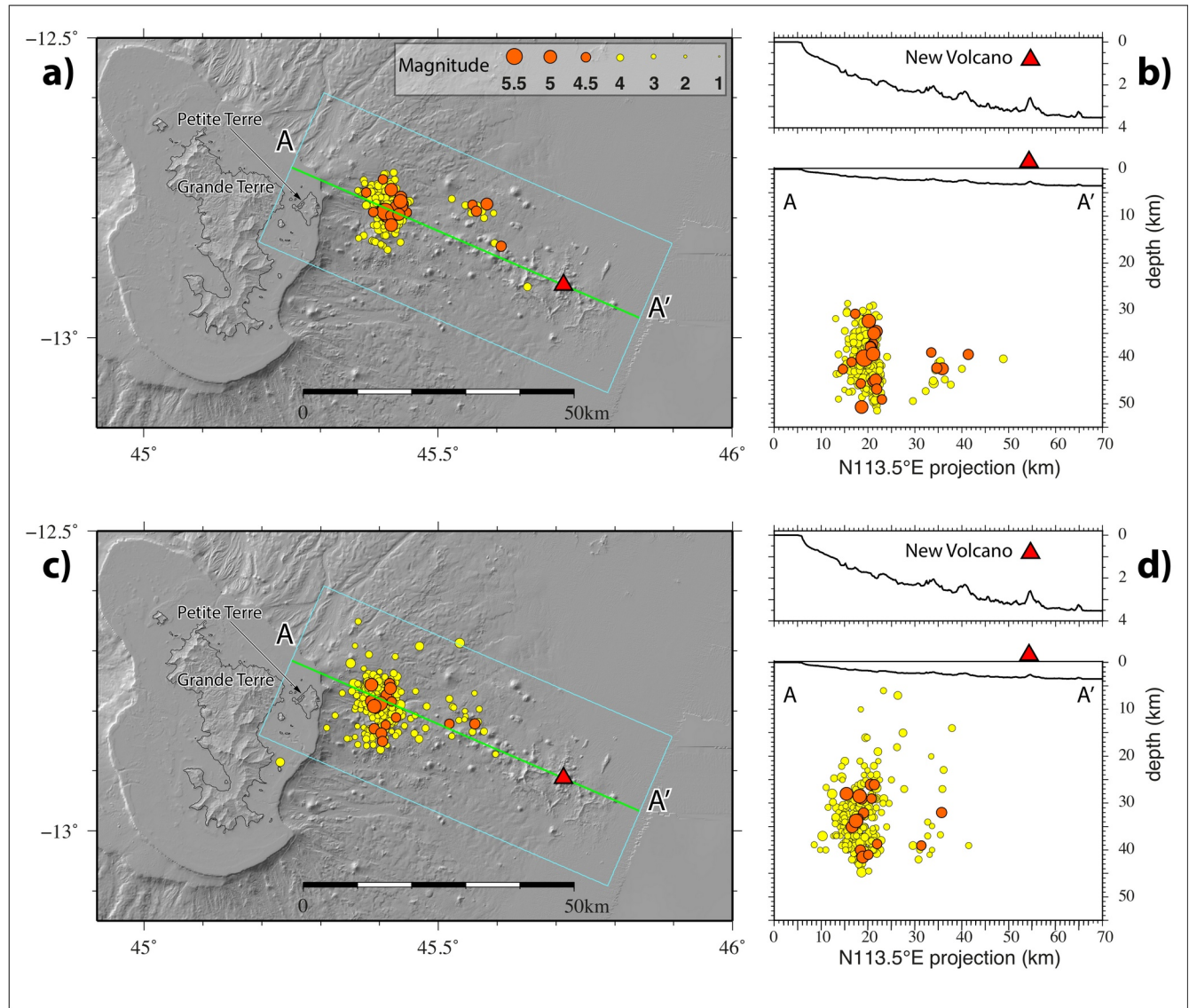


Figure S2 : a) and b) : map and cross-section of this study catalog (OBS locations with hybrid ADofal velocity model). c) and (d) : map and cross-section of the same earthquakes from Lemoine et al (2020) catalog with land-based seismic stations.

Proximal and Distal clusters can be distinguished in both catalogs. While there is not much differences in the location of the Proximal cluster, the Distal cluster is located 5 to 10 km north of Lemoine's catalog with the OBS data. Earthquakes depths are also better constrained, as expected, with the OBS network. Distal cluster seems also more tightly oriented toward the volcano with the OBS, which match the dyke interpretation of this cluster from Lemoine et al (2020). During this 2.5 months period, there are 321 earthquakes in Lemoine et al (2020) catalog and 2131 in this study catalog.

Earthquake density map

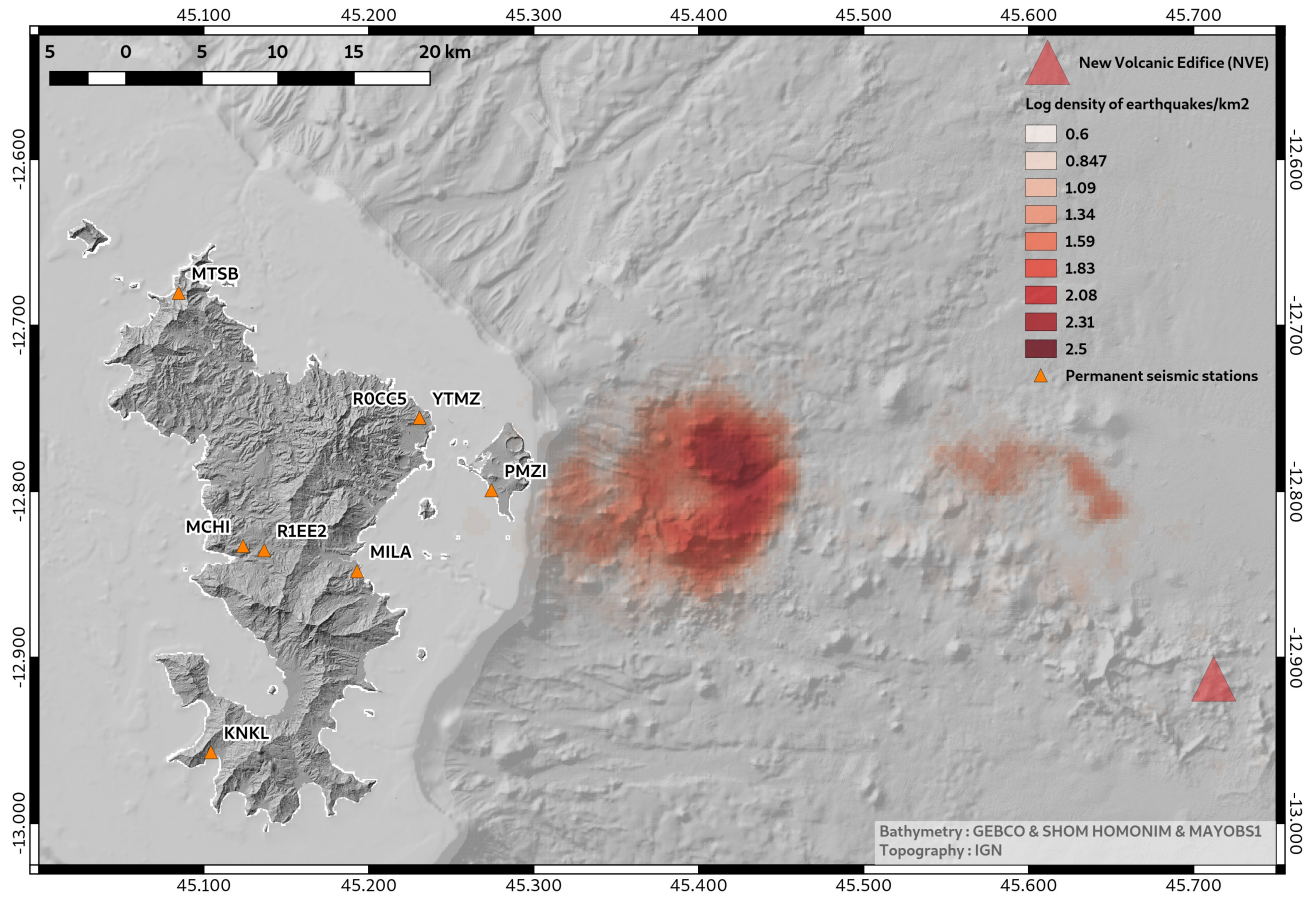


Figure S3 : map of the log₁₀ density of earthquakes. Density calculated using QGIS heatmap plugin, a 0.01 degree radius and uniform kernel. The Proximal cluster, which has a donut shape, appears to have a high density of events in its north-east side.